ChemComm

Check for updates

ROYAL SOCIETY OF CHEMISTRY

Facile preparation of a Ni–imidazole compound with high activity for ethylene dimerization†

Zhaohui Liu,[a] Guanxing Li,[b] Mohammed R. Alalouni,[c] Ziyin Chen,[d] Xinglong Dong, [ID] *[e] Jianjian Wang [ID] [a] and Cailing Chen [ID] *[b]

A compound consisting of Ni and imidazole (Ni–imidazole) was synthesized in large quantities by a one-step co-precipitation method. The structure and stability of this Ni–imidazole were well studied by a series of characterization methods. The Ni–imidazole compound exhibited excellent catalytic properties for the dimerization of ethylene to 1-butene.

As an important linear α-olefin, 1-butene is widely used in industry to produce unique polymers with enhanced mechanical strength and thermal stability.[1] Nowadays, 1-butene is mainly produced from crude oil cracking, ethylene oligomerization and dimerization.[2] Considering the ever-increasing consumption of crude oil and the high product selectivity, the ethylene dimerization technology has gained the highest market share.[3]

The commercial process of ethylene dimerization is currently using homogeneous catalysts. Although their high activity and selectivity are attractive, many shortcomings of these commercial catalysts cannot be ignored.[3] For instance, their lifetime is usually shorter than a few hours;[4] meanwhile, the costly separation procedure of the catalysts and products is complicated and energy consuming;[5] in addition, unexpected polymeric byproducts associated with the reaction would foul the heat exchanger

and the reactor.[1] Therefore, the exploration of heterogeneous catalytic alternatives is highly desirable.

Many nanosized metal catalysts supported on oxides or zeolites have been tested for the ethylene dimerization reaction. However, due to the high mobility of metal species and the detrimental metal–support interaction, they exhibited much lower activities than the homogeneous catalysts.[6–9] In comparison, MOF-based catalysts, with structural tunability and high porosity, have attracted much attention and shown outstanding performance for ethylene dimerization.[10–15] Canivet *et al.* first prepared a Ni@(Fe)MIL-101 catalyst *via* anchoring nickel complexes on MOF frameworks, which gave a turnover frequency (TOF, moles of ethylene consumed per mole of active sites per unit time) of 20 910 h^{-1}, corresponding to 205 grams of butene per gram of Ni@(Fe)MIL-101 per hour.[10] Metzger *et al.* synthesized a Ni-MFU-4l catalyst featuring the active Ni^{2+} sites similar to the [Tp^{Mes}Ni]$^{+}$ complexes, which showed a high TOF of 41 500 h^{-1} in a 1 h batch reaction performed at 25 °C and 50 bar.[11]

Recently, we designed a Ni-ZIF-8 catalyst with 0.7 wt% Ni loading, in which Ni sites were selectively anchored on the surface of the particles. Its activity with a TOF of 297 000 h^{-1} exceeded all previously reported heterogeneous catalysts and most homogeneous catalysts.[16] Subsequently, another Ni-ZIF-L catalyst with 0.49 wt% Ni loading was also developed in our group, which showed an even higher activity with a TOF of 330 320 h^{-1}.[17] However, we realized that the Ni loading amount correlated with the external surface area of the support determined the overall performance of these catalysts.

Although TOF is an important value to indicate the activity of the catalytic site, the mass activity of the entire catalyst is more relevant in real industrial production. Increasing the loading amount of Ni sites in the catalyst while maintaining a high TOF value is still challenging for the ethylene dimerization reaction. Bearing that in mind, we then developed a series of Ni-MOF-5 catalysts, among which the 20Ni-MOF-5 catalyst with 5.32 wt% Ni loading achieved a TOF of 352 000 h^{-1} at 35 °C and 50 bar, corresponding to 9040 grams of product per gram of

[a] *School of Chemistry and Chemical Engineering & Institute of Advanced Interdisciplinary Studies, Multi-scale Porous Materials Center, Chongqing University, Chongqing, 401331, China*

[b] *Advanced Membranes and Porous Materials (AMPM) Center, Physical Sciences and Engineering Division, King Abdullah University of Science and Technology (KAUST), Thuwal 23955, Saudi Arabia. E-mail: cailing.chen@kaust.edu.sa*

[c] *Catalyst Center of Excellence (CCoE), Research and Development Center, Saudi Aramco, Dhahran 31311, Saudi Arabia*

[d] *Gas and Particulate Metrology Group, National Physical Laboratory, Teddington, London TW11 0LW, UK*

[e] *School of Chemistry, University of Lincoln, Brayford Pool, Lincoln, LN6 7TS, UK. E-mail: xinglong.dong.uk@gmail.com*

† Electronic supplementary information (ESI) available. See DOI: https://doi.org/10.1039/d3cc04794f

catalyst per hour.[18] This mass activity achieved by the 20Ni-MOF-5 catalyst exceeded all previously reported heterogeneous catalysts.

Even though lots of efforts have recently been made, it is yet a great challenge to find a low-cost, easy-to-prepare and high-performance heterogenous catalyst for commercial application in ethylene dimerization. In this report, a Ni–imidazole compound was synthesized in large quantities ($\sim$20 g in one batch) by a simple one-step co-precipitation method, which achieved 6378 grams of product per gram of catalyst per hour at 50 °C and 30 bar, exceeding the mass activity of the 20Ni-MOF-5 catalyst under the same reaction conditions. The structural properties of this Ni–imidazole were well studied to reveal its unique performance. The simple preparation method together with the prominent performance enables the great potential of the Ni–imidazole catalyst for industrial ethylene dimerization.

The Ni–imidazole compound was synthesized by a very simple and green one-step co-precipitation method using water as the solvent at room temperature, as shown in Fig. 1a. A typical procedure is as follows. 2 mmol of nickel nitrate and 12 mmol of imidazole were dissolved in 5 ml of water to form solution A and solution B, respectively. By quickly mixing solution A with solution B, a purple liquid can be obtained, and then a purple precipitate was obtained by standing for 5 min, and finally the purple Ni–imidazole compound can be obtained by filtering out the solution. Expanding the reaction by a factor of 15 in equal proportions still gave pure nickel imidazole compounds, as shown in Fig. 1b, with a mass of about 19.58 g obtained each time. The crystallinity and structure of the obtained products were studied by powder X-ray diffraction (XRD). The red curve in Fig. 1c is the simulated XRD pattern that has been reported for Ni–imidazole compounds, while the black curve is the experimentally obtained XRD pattern. It is certainly confirmed that the experimentally obtained XRD pattern matches the reported one perfectly. To further clarify the structure of this compound, we did Rietveld refinement on the obtained powder XRD (Fig. S1, ESI†). The structure of the Ni–imidazole compound is schematically shown in Fig. 1d.

The Ni–imidazole crystal is composed of Ni^{2+} coordinated to six imidazole groups, and the NO_3^- group is added to balance the charge (formula: $NiC_{18}N_{14}O_6H_{24}$), which is indexed to a trigonal $R\bar{3}$ space group with a = 12.36 Å and c = 14.81 Å. Beyond getting the Ni–imidazole compound, this simple green one-step precipitation method can be extended to synthesize Co-imidazole compounds by simply replacing nickel nitrate in the precursor with cobalt nitrate (Fig. S2, ESI†).

As shown in Fig. 2a, the morphology and structure of Ni–imidazole were further observed by transmission electron microscopy (TEM). From the low magnification TEM image, Ni–imidazole crystals have a regular shape. To avoid structural damage of the sample under an electron beam, we used an ultra-low electron dose TEM technique to obtain a high-resolution TEM image of Ni–imidazole, and the lattice fringes can be clearly observed by measuring the d-space of 0.87 nm ascribed to the (101) reflection. Fig. 2b shows the high-angle annular dark-field scanning transmission electron microscopy (HAADF-STEM) image and the corresponding energy-dispersive X-ray spectroscopy (EDS) elemental maps of Ni–imidazole, indicating a uniform distribution of the elements Ni, N, C and O. To test the thermal stability of Ni–imidazole, a thermogravimetric analysis was then performed (Fig. 2c). The 4.95% of the weight loss that begins at about 70 °C is supposed to be water and other species adsorbed by the sample. There is a large amount of weight loss (40.61%) in the sample from 180 °C indicating that the sample is decomposed. X-ray photoelectron spectroscopy (XPS) was used to characterize the elemental states. The XPS survey scan (Fig. S3, ESI†) indicates that Ni–imidazole contains Ni, N, C and O elements, which is consistent with the EDS results. The high-resolution XPS of Ni 2p, as shown in Fig. 2d, exhibits the main peaks of $2P_{3/2}$ (855 eV) and $2P_{1/2}$ (872 eV) and their corresponding shake up satellite peaks, demonstrating Ni^{2+} in the Ni–imidazole compound.[19]

Most heterogeneous catalysts used in current studies of catalytic ethylene dimerization to produce 1-butene are Ni catalysts, and therefore the synthesized Ni–imidazole was
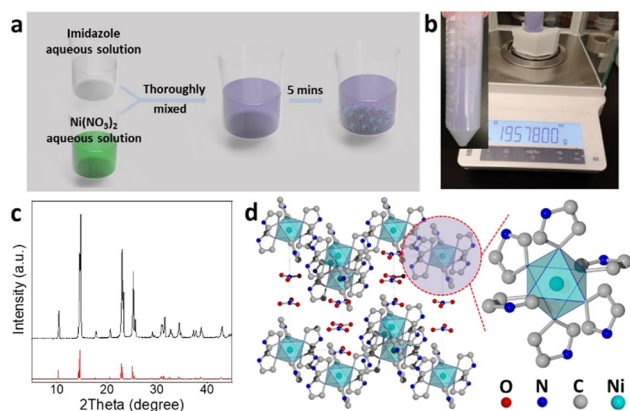

Fig. 1 (a) Schematic diagram of the synthetic Ni–imidazole catalyst. (b) Photograph of Ni–imidazole under sunlight. (c) and (d) XRD patterns and structural model of Ni–imidazole.
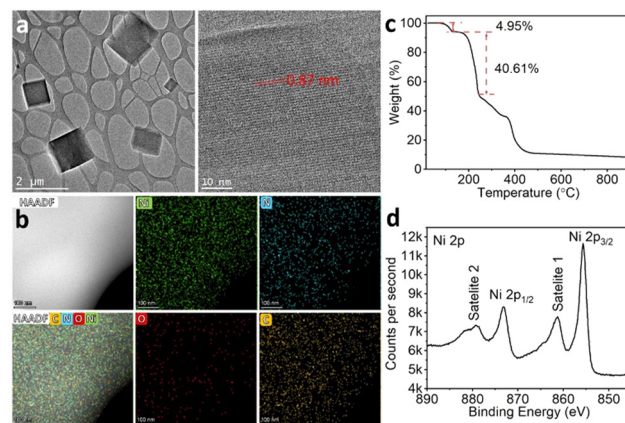

Fig. 2 (a) TEM images, (b) HAADF-STEM image and the corresponding EDS maps, (c) high resolution XPS spectra for the Ni 2p and (d) TGA profile of Ni–imidazole.

ChemComm

Table 1 Ethylene dimerization catalyzed by the Ni–imidazole compound

Entry[a]	TOF[b] ($mol_{C_2H_4}\ mol_{Ni}^{-1}\ h^{-1}$)	Activity[c] ($g_{product}\ g_{cata}^{-1}\ h^{-1}$)	Selectivity[d]	MAO conc. (mol L^{-1})	P. (bar)	T. (°C)
1	119 198	4 525	C4 = 92.0% (1-C4 = 75.5%)	0.075	30	35
2	0	0	0	0	30	35
3	19 583	743	C4 = 93.0% (1-C4 = 90.5%)	0.015	30	35
4	51 378	1 950	C4 = 92.6% (1-C4 = 86.2%)	0.0375	30	35
5	151 648	5 757	C4 = 91.6% (1-C4 = 72.8%)	0.150	30	35
6	156 533	5 943	C4 = 86.1% (1-C4 = 68.8%)	0.225	30	35
7	31 928	1 212	C4 = 97.1% (1-C4 = 96.7%)	0.075	30	0
8	98 262	3 731	C4 = 96.4% (1-C4 = 77.4%)	0.075	30	R.T.
9	167 195	6 378	C4 = 85.0% (1-C4 = 62.1%)	0.075	30	50
10	12 708	482	C4 = 90.5% (1-C4 = 75.1%)	0.075	5	35
11	37 664	1 430	C4 = 91.1% (1-C4 = 75.9%)	0.075	10	35
12	82 218	3 121	C4 = 91.9% (1-C4 = 75.2%)	0.075	20	35

[a] Catalyst amount: 5 mg; solvent: 20 ml of toluene; reaction time: 10 min. [b] Moles of ethylene consumed per mole of Ni per hour. [c] Grams of product per gram of catalyst per hour. [d] The 1-C4 selectivity refers to the percentage of 1-butene in the C4 products.

proposed to catalyze ethylene dimerization. We evaluated the catalytic performance of Ni–imidazole using a liquid-phase batch reactor, toluene as a solvent and methylaluminoxane (MAO) as a co-catalyst. A typical reaction procedure is as follows, 5 mg of dried Ni–imidazole, 20 ml of dried toluene and 1 ml of MAO (10 wt% Al in toluene solution) loaded into 75 ml of Parr autoclave in a glove box, sealed and transferred out of the glove box, followed by a 10 min reaction at 35 °C under a continuous flow of 30 bar of ethylene (entry 3 in Table 1 and Fig. S4, ESI†). As shown in Fig. S5 (ESI†), without Ni–imidazole, the gas chromatography (GC) record did not detect any peaks for butenes, indicating that the catalytic reaction could not proceed.

In addition, as shown in entry 1 of Table 1, MAO is essential in this reaction, and the ethylene dimerization reaction cannot occur without the addition of the co-catalysts. As can be seen from entries 1–6 in Table 1, the catalytic activity increases with MAO concentration increasing. To analyze the effect of MAO on the catalytic reaction performance in detail, we plotted the concentration of MAO *versus* catalytic activity and selectivity (Fig. S6, ESI†). The catalytic activity shows a linear increase with MAO until 0.075 mol L^{-1}, after which the increase slows down. The increase in catalytic activity is because the catalyst Ni–imidazole has more contact chance by more MAO. A high concentration of MAO increases the probability of Ni–imidazole being activated, so the catalytic activity increases accordingly. But the catalytic activity will not always increase rapidly because a certain amount of catalyst is needed for only a certain amount of co-catalyst MAO.

However, the selectivity of either butenes (C4) or 1-butene (1-C4) decreases with increasing the concentration of MAO. With the increase of activity, 1-C4 in the system cannot be removed from the reactive site in time, so that 1-C4 continues to react as a reactant to a trimerization product or an isomerization product, and thus the selectivity of C4 and 1-C4 decreases. In order to maintain high activity and selectivity, here we chose the concentration of MAO 0.075 mol L^{-1} as a standard for the study of other factors in the reaction. As shown in entries 1 and entries 7–9 in Table 1, the catalytic activity increases with increasing temperature because increasing

temperature increases the probability of collisions between molecules thereby increasing the probability of contact between the catalytic active sites and reactant molecules. As expected, the selectivity of 1-C4 and C4, on the other hand, declines with increasing catalytic activity, especially at 50 °C, where the selectivity of C4 is only 85.0% and the selectivity of 1-C4 in C4 drops to 62.1% (Fig. S7, ESI†).

We also investigated the effect of reactant concentration, that is, the pressure of ethylene, on catalytic activity and selectivity. With increasing ethylene pressure, the catalytic activity increases, and the selectivity of C4 increases, and the selectivity of 1-C4 in C4 remains almost stable, indicating that higher pressures are more favorable to the reaction (entries 1 and entries 10–12 in Table 1 and Fig. S8, ESI†). The reason is that the higher the pressure of the ethylene the greater the possibility of contact with the active site, so the activity is higher. The reason that the selectivity does not decrease with higher activity is that ethylene and 1-butene are in a competitive relationship throughout the system. The higher the concentration of ethylene, the smaller the possibility of contact between 1-butene and the active site. Therefore, the possibility of trimerization or isomerization decreases, while the selectivity of C4 remains a high value. Although, in agreement with the previous reports, high pressures are beneficial for the reaction, we used a maximum ethylene pressure of 30 bar in this study for safety reasons due to the high activity of the catalysts.[10]

To further demonstrate the superiority of this catalyst, we compared the reported activities of some typical heterogeneous catalysts for ethylene dimerization with that of the as-obtained Ni–imidazole.[10,11,14–18,20–29] The TOF of Ni–imidazole can reach up to 167 195 ethylene moles of ethylene consumed per mole of Ni per hour at 30 bar, which exceeds the activity of most heterogeneous catalysts under similar conditions, but is lower than our previously reported ZIF catalyst activity (Fig. S9, ESI†). However, in practice, more attention is paid to the activity per unit of catalyst (*e.g.*, mass activity of the catalyst) rather than per unit of Ni. Due to the high Ni content in Ni–imidazole, the mass activity can be as high as 6378 grams of product per gram of Ni–imidazole per hour at 30 bar ethylene, which surpasses

the 20Ni-MOF-5 catalyst under the same reaction conditions (Fig. S10, ESI†).

The catalytic mechanism is crucial for a catalytic reaction. Exploring the reaction mechanism can help us further understand the nature of the catalytic reaction. There are two proposed processes for catalytic ethylene dimerization, one is the metallacycle mechanism and the other is the Cossee–Arlman mechanism (Fig. S11, ESI†).[30,31] The metallacycle mechanism involves the simultaneous coordination of two ethylenes to the active metal site to form metallocyclopentane, which then decomposes to produce 1-butene. In contrast, the Cossee–Arlman mechanism involves the insertion of two ethylenes sequentially into the metal active site to form a metallobutyl chain, which is then chain transferred to produce 1-butene. The metallacycle mechanism and Cossee–Arlman mechanism can be distinguished by designing an isotope labeling experiment (Fig. S12, ESI†). Isotope products can be distinguished by analyzing their fragmentation peaks using mass spectrometry. Therefore, the reaction mechanism of ethylene dimerization over Ni–imidazole is analyzed by utilizing the established methodology.[16,31] Fig. S11 (ESI†) shows the comparison of 1-butene fragmentation patterns from a mixed $1:1$ C_2H_4/C_2D_4 gas based on experimental results and predictions from the proposed metallacycle and Cossee–Arlman mechanisms, which suggest that the experimental results are more consistent with those predicted by the Cossee–Arlman mechanism, especially for fragmentation peaks with m/z of 57, 59, 61 and 63. The reaction follows the Cossee–Arlman mechanism which also explains that 1-butene undergoes isomerization to 2-butenes (Fig. S5, ESI†).

In summary, we synthesized a Ni–imidazole compound by a simple one-step precipitation method at room temperature using Ni nitrate and imidazole as source materials and water as solvent. The structure and stability of this compound were investigated in detail. To evaluate the catalytic properties, this compound was used in the catalytic reaction for the dimerization of ethylene to produce 1-butene and showed excellent catalytic performance. Due to the high nickel loading and TOF, the mass activity of 6378 grams of product per gram of catalyst per hour surpasses that of most heterogeneous catalysts. The simplicity of the synthesis and the good properties make this Ni–imidazole compound highly promising for industrial catalytic ethylene dimerization.

Conflicts of interest

There are no conflicts to declare.

Notes and references

1 M. Sturzel, S. Mihan and R. Mulhaupt, *Chem. Rev.*, 2016, **116**, 1398–1433.
2 M. Bender, *ChemBioEng Rev.*, 2014, **1**, 136–147.
3 H. Olivier-Bourbigou, P. A. R. Breuil, L. Magna, T. Michel, M. F. Espada Pastor and D. Delcroix, *Chem. Rev.*, 2020, **120**, 7919–7983.
4 A. W. Al-Sa'doun, *Appl. Catal., A*, 1993, **105**, 1–40.
5 V. Hulea, *ACS Catal.*, 2018, **8**, 3263–3279.
6 E. Angelescu, M. Che, M. Andruh, R. Zăvoianu, G. Costentin, C. Mirică and O. Dumitru Pavel, *J. Mol. Catal. A: Chem.*, 2004, **219**, 13–19.
7 E. Rossetto, B. P. Nicola, R. F. de Souza, K. Bernardo-Gusmão and S. B. C. Pergher, *J. Catal.*, 2015, **323**, 45–54.
8 J. R. Sohn and S. Y. Lee, *Appl. Catal., A*, 1997, **164**, 127–140.
9 M. Lallemand, A. Finiels, F. Fajula and V. Hulea, *Stud. Surf. Sci. Catal.*, 2007, **170**, 1863–1869.
10 J. Canivet, S. Aguado, Y. Schuurman and D. Farrusseng, *J. Am. Chem. Soc.*, 2013, **135**, 4195–4198.
11 E. D. Metzger, C. K. Brozek, R. J. Comito and M. Dinca, *ACS Cent. Sci.*, 2016, **2**, 148–161.
12 U. S. F. Arrozi, V. Bon, S. Krause, T. Lubken, M. S. Weiss, I. Senkovska and S. Kaskel, *Inorg. Chem.*, 2020, **59**, 350–359.
13 X. N. Wang, P. Zhang, A. Kirchon, J. L. Li, W. M. Chen, Y. M. Zhao, B. Li and H. C. Zhou, *J. Am. Chem. Soc.*, 2019, **141**, 13654–13663.
14 Y. Hu, Y. Zhang, Y. Han, D. Sheng, D. Shan, X. Liu and A. Cheng, *ACS Appl. Nano Mater.*, 2018, **2**, 136–142.
15 E. D. Metzger, R. J. Comito, Z. Wu, G. Zhang, R. C. Dubey, W. Xu, J. T. Miller and M. Dincă, *ACS Sustainable Chem. Eng.*, 2019, **7**, 6654–6661.
16 C. Chen, M. R. Alalouni, X. Dong, Z. Cao, Q. Cheng, L. Zheng, L. Meng, C. Guan, L. Liu, E. Abou-Hamad, J. Wang, Z. Shi, K.-W. Huang, L. Cavallo and Y. Han, *J. Am. Chem. Soc.*, 2021, **143**, 7144–7153.
17 C. Chen, M. R. Alalouni, P. Xiao, G. Li, T. Pan, J. Shen, Q. Cheng and X. Dong, *Ind. Eng. Chem. Res.*, 2022, **61**, 14374–14381.
18 C. Chen, L. Meng, M. R. Alalouni, X. Dong, Z. P. Wu, S. Zuo and H. Zhang, *Small*, 2023, **19**, 2301235.
19 A. Kotta, E. B. Kim, S. Ameen, H. S. Shin and H. K. Seo, *J. Electrochem. Soc.*, 2020, **167**, 167517.
20 E. Rozhko, A. Bavykina, D. Osadchii, M. Makkee and J. Gascon, *J. Catal.*, 2017, **345**, 270–280.
21 U. S. F. Arrozi, V. Bon, C. Kutzscher, I. Senkovska and S. Kaskel, *Dalton Trans.*, 2019, **48**, 3415–3421.
22 R. D. Andrei, M. L. Popa, F. Fajula and V. Hulea, *J. Catal.*, 2015, **323**, 76–84.
23 S. T. Madrahimov, J. R. Gallagher, G. H. Zhang, Z. Meinhart, S. J. Garibay, M. Delferro, J. T. Miller, O. K. Farha, J. T. Hupp and S. T. Nguyen, *ACS Catal.*, 2015, **5**, 6713–6718.
24 L. Chen, Y. Jiang, H. Huo, J. Liu, Y. Li, C. Li, N. Zhang and J. Wang, *Appl. Catal., A*, 2020, **594**, 117457.
25 M. Lallemand, O. A. Rusu, E. Dumitriu, A. Finiels, F. Fajula and V. Hulea, *Appl. Catal., A*, 2008, **338**, 37–43.
26 M. Lallemand, A. Finiels, F. Fajula and V. Hulea, *Appl. Catal., A*, 2006, **301**, 196–201.
27 M. I. Gonzalez, J. Oktawiec and J. R. Long, *Faraday Discuss.*, 2017, **201**, 351–367.
28 A. Lacarriere, J. Robin, D. Swierczynski, A. Finiels, F. Fajula, F. Luck and V. Hulea, *ChemSusChem*, 2012, **5**, 1787–1792.
29 S. Yuan, P. Zhang, L. Zhang, A. T. Garcia-Esparza, D. Sokaras, J. S. Qin, L. Feng, G. S. Day, W. Chen, H. F. Drake, P. Elumalai, S. T. Madrahimov, D. Sun and H. C. Zhou, *J. Am. Chem. Soc.*, 2018, **140**, 10814–10819.
30 F. Speiser, P. Braunstein and L. Saussine, *Acc. Chem. Res.*, 2005, **38**, 784–793.
31 E. D. Metzger, R. J. Comito, C. H. Hendon and M. Dinca, *J. Am. Chem. Soc.*, 2017, **139**, 757–762.